Residue-Specific Effects on Slow Inactivation at V787 in D2-S6 of $Na_v1.4$ Sodium Channels

John P. O'Reilly,* Sho-Ya Wang,† and Ging Kuo Wang*
*Department of Anesthesia Research, Brigham and Women's Hospital, Harvard Medical School, Boston, Massachusetts 02115; and †Department of Biological Sciences, State University of New York at Albany, Albany, New York 12222 USA

ABSTRACT Slow inactivation in voltage-gated sodium channels (NaChs) occurs in response to depolarizations of seconds to minutes and is thought to play an important role in regulating membrane excitability and action potential firing patterns. However, the molecular mechanisms of slow inactivation are not well understood. To test the hypothesis that transmembrane segment 6 of domain 2 (D2-S6) plays a role in NaCh slow inactivation, we substituted different amino acids at position V787 (valine) in D2-S6 of rat skeletal muscle NaCh μ1 ($Na_v1.4$). Whole-cell recordings from transiently expressed NaChs in HEK cells were used to study and compare slow inactivation phenotypes between mutants and wild type. V787K (lysine substitution) showed a marked enhancement of slow inactivation. V787K enters the slow-inactivated state $\approx$100$\times$ faster than wild type ($\tau_1 \approx$ 30 ms vs. $\approx$3 s), and occurs at much more hyperpolarized potentials than wild type ($V_{1/2}$ of s_∞ curve ≈ -130 mV vs. ≈ -75 mV). V787C (cysteine substitution) showed a resistance to slow inactivation, i.e., opposite to that of V787K. Entry into the slow inactivation state in V787C was slower ($\tau_1 \approx$ 5 s), less complete, and less voltage-dependent ($V_{1/2}$ of s_∞ curve ≈ -50 mV) than in wild type. Application of the cysteine modification agent methanethiosulfonate ethylammonium (MTSEA) to V787C demonstrated that the 787 position undergoes a relative change in molecular conformation that is associated with the slow inactivation state. Our results suggest that the V787 position in $Na_v1.4$ plays an important role in slow inactivation gating and that molecular rearrangement occurs at or near residue V787 in D2-S6 during NaCh slow inactivation.

INTRODUCTION

Voltage-gated Na^+ channels (NaChs) open and inactivate in response to depolarization of the membrane potential. Many investigators have actively pursued an understanding of this response using a variety of techniques (Hodgkin and Huxley, 1952; Armstrong et al., 1973; Aldrich et al., 1983; Stuhmer et al., 1989). In an effort to understand the molecular mechanisms underlying this process, recent studies have used NaCh clones from several excitable tissues. The sequencing and functional expression of these clones have shown that the α-subunit of NaChs (Fig. 1) comprises four homologous domains (D1-D4), each with six transmembrane segments (S1-S6), and that the α-subunit appears to be sufficient for activation, inactivation, and ion selectivity (Noda et al., 1984, 1986; Trimmer et al., 1989; Gellens et al., 1992). In particular, studies using site-directed mutagenesis have assigned specific functions to specific regions of NaChs. For example, the voltage sensors for activation of NaChs are believed to be in the S4 transmembrane segments (Stuhmer et al., 1989), whereas the cytoplasmic linker between D3 and D4, along with the S4-S5 loop in D3 and/or D4 appears to be the fast-inactivation gate (Patton et al., 1992; Smith and Goldin, 1997; McPhee et al., 1998). The outer pore of the NaCh is probably formed by the P-segments (i.e., the SS1-SS2 regions between S5 and S6), which also play a prominent role in Na^+ ion selectivity (Heinemann et al., 1992), while the inner pore may be lined by the S6 segments (Lipkind and Fozzard, 2000). Also of interest is that mutations in S6 can have dramatic effects on gating in NaChs (Yarov-Yarovoy et al., 2001). In particular, the S6 segments may play an important role in slow inactivation gating (Cannon and Strittmatter, 1993; Wang and Wang, 1997; Hayward et al., 1997; Takahashi and Cannon, 1999; Vedantham and Cannon, 2000).

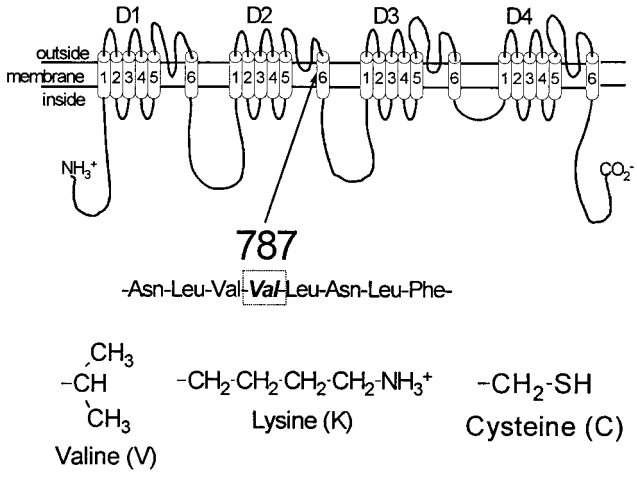

FIGURE 1 The α-subunit of the voltage-gated Na^+ channel. A diagram of the α-subunit of the rat skeletal muscle Na^+ channel showing the four domains (D1-D4) each with six transmembrane segments (S1-S6). The 787 residue is located in D2-S6 (a partial amino acid sequence is shown with the native valine residue at 787 in the box). The side chains of the native valine (V) and the amino acid substitutions of lysine (K) and cysteine (C) are also presented.

Received for publication 1 June 2001 and in final form 12 July 2001.

Address reprint requests to John P. O'Reilly, Ph.D., Department of Anesthesia Research, Brigham and Women's Hospital, Harvard Medical School, 75 Francis Street, Boston, MA 02115. Tel.: 617-732-6883; Fax: 617-730-2801; E-mail: joreilly@zeus.bwh.harvard.edu.

0006-3495/01/10/2100/12 $2.00

Slow inactivation in NaChs is a nonconducting, conformational state that is kinetically and molecularly distinct from fast inactivation. Slow inactivation occurs over a time scale of seconds to minutes and is thought to be important in membrane excitability and action potential firing patterns (Ruff et al., 1988; Sawczuk et al., 1995). In contrast, fast inactivation occurs within milliseconds of membrane depolarization and plays an important role in the termination of action potentials (Hille, 1992). Slow inactivation is believed to be dependent on different molecular mechanisms from fast inactivation because manipulations that eliminate fast inactivation, e.g., internal perfusion with protease or amino acid substitutions in the D3-D4 linker, fail to eliminate slow inactivation (Rudy, 1978; Featherstone et al., 1996).

Disruption of NaCh inactivation has been implicated in several human diseases. For example, in the human heart, inheritable NaCh mutations that alter fast inactivation produce long QT syndrome (Wang et al., 1996) and mutations that alter slow inactivation in the human skeletal muscle NaCh produce hyperkalemic periodic paralysis (Cummins and Sigworth, 1996; Hayward et al., 1997). Therefore, understanding the molecular basis of NaCh inactivation can have important clinical implications.

In this study we have characterized NaCh mutants that have amino acid substitutions for the native valine (V) at position 787 in domain 2, segment 6 (D2-S6) of wild-type rat skeletal muscle NaCh μ1 ($Na_v1.4$) (Trimmer et al., 1989) (Fig. 1). We studied these mutants to test the hypothesis that D2-S6 of NaChs plays an important role in slow inactivation gating. We chose D2 because our previous study with NaCh chimeras suggested that this domain plays a prominent role in slow inactivation gating (O'Reilly et al., 1999). We studied position 787 because this region of S6 appears to be involved in the slow inactivation process (Wang and Wang, 1997; Vedantham and Cannon, 2000).We used patch-clamp techniques on transiently transfected HEK cells to compare the activation and inactivation kinetics between mutants and wild type. We found marked and opposite effects on the slow inactivation phenotype between two of the mutants and wild type: V787K showed a marked enhancement of slow inactivation, while V787C showed a resistance to slow inactivation. In addition, slow inactivation produces a relative change in the molecular position of the V787 residue as monitored in V787C by application of the cysteine modification agent methanethiosulfonate ethylammonium (MTSEA). Our results suggest that the V787 position in D2-S6 plays an important role in slow inactivation gating of NaChs. We propose that a molecular conformational change during depolarization alters the relative position of the V787 residue. We hypothesize that the positively charged lysine substitution in V787K rapidly stabilizes the slow inactivation state, whereas in V787C the slow inactivation state is relatively unstable due to differences in the three-dimensional structure of the substituted amino acid side chain at the V787 position.

MATERIALS AND METHODS

Na^+ channel (NaCh) mutant construction and transient transfection of cDNA clones

Mutants were produced with amino acid substitutions in wild type rat skeletal muscle NaCh μ1 ($Na_v1.4$) (Trimmer et al., 1989) as described previously (Wang and Wang, 1997). cDNA clones of wild-type and NaCh mutants were transiently transfected into HEK293t cells using the calcium phosphate precipitation method (Graham and Eb, 1973) as previously described (O'Reilly et al., 1999). The transfection included 0.5 μg of CD8 (cell surface antigen) and 5–10 μg of NaCh cDNA subcloned in the pcDNA1/amp vector (Invitrogen, San Diego, CA).

Recording techniques

We used standard patch-clamp techniques (Hamill et al., 1981) to record whole-cell peak Na^+ current (I_{Na}) from transiently transfected HEK293t cells. Recordings were performed at room temperature (20–22°C) and no correction was made for liquid junction potentials. Conductance-voltage (activation) and steady-state fast inactivation (h_∞) curves were obtained ≈10 min after rupture of the membrane. Recording micropipettes (Drummond Scientific, Broomall, PA) were pulled on a Model P-87 Flaming-Brown puller (Sutter Instruments, Novato, CA). Pipette resistance ranged from 0.5 to 1.5 MΩ when measured in our solutions. The extracellular recording solution was (in mM): 65 NaCl, 85 choline-Cl, 2 $CaCl_2$ and 10 HEPES, titrated to pH 7.4 with TMA-OH. The pipette (intracellular) solution was (in mM): 100 NaF, 30 NaCl, 10 EGTA, and 10 HEPES, titrated to pH 7.2 with CsOH. These solutions create an outward Na^+ gradient and an outward Na^+ current at the test pulse of +50 mV reducing potential problems associated with space clamp or series resistance errors (Cota and Armstrong, 1989). Series resistance was compensated at 80%, resulting in voltage errors of <5 mV. Linear leak subtraction based on five hyperpolarizing pulses was used for all recordings. Any endogenous K^+ currents were blocked with Cs^+ in the pipette, and HEK cells express no native Ca^{2+} current (Ukomadu et al., 1992). Cells were selected for recording based on positive immunoreaction with CD8 Dynabeads (Dynal Biotech, Inc., Lake Success, NY).

Electrophysiology protocols

Activation and fast inactivation

The holding potential (V_{hold}) was −160 mV for wild type and all mutants except V787K. V_{hold} for V787K was increased to −200 mV because of the enhanced voltage-dependence of inactivation for this mutant (e.g., see Fig. 5 *A*). A test pulse to +50 mV (4 ms) was used to record peak available Na^+ current (I_{Na}). Activation and fast inactivation curves (h_∞) were obtained using standard protocols and fit with Boltzmann functions as previously described (O'Reilly et al., 1999).

Recovery from short depolarizations

Recovery from short depolarizations was determined with a two-pulse protocol: a prepulse step to 0 mV for 8 or 100 ms, a step to V_{hold} for variable recovery times (0.2 ms–60 s), then the test pulse to +50 mV (4 ms). Identical results are found with prepulse depolarizations of +30 or +50 mV (data not shown). The peak current recorded with the test pulse was normalized to I_{Na} obtained after 60 s at V_{hold}. The time at V_{hold} between pulses was >10 s (>60 s for V787K). The mean data were fit with the double-exponential function: $I/I_{max} = I_0 + A_1(1 - \exp(-x/\tau_1)) + A_2(1 - \exp(-x/\tau_2))$, where I_0 is the non-inactivating component, I_{max} is the peak current, x is time, and A_1 and A_2 are the components for the time constants τ_1 and τ_2, respectively.

Slow inactivation

To produce slow inactivation, the voltage was stepped to 0 mV. Preliminary experiments verified that there was no significant difference in the development of slow inactivation with larger voltage steps (up to +30 mV). Cells were held at V_{hold} for >2 min between pulses during the slow inactivation protocols. Also, I_{Na} was checked between pulses to check for possible time-dependent cumulative effects. Three protocols were used to determine slow inactivation phenotype:

Development of slow inactivation. Voltage was stepped from V_{hold} to 0 mV for various times (1 ms–120 s), stepped to V_{hold} for 50 ms to allow recovery from fast inactivation, and then stepped to +50 mV (4 ms) to record I_{Na}. I_{Na} was normalized to the initial value recorded before the start of the protocol. Data were fit with a double-exponential function: $I/I_{max} = I_0 + A_1\exp(-x/\tau_1) + A_2\exp(-x/\tau_2)$, where I_0, I_{max}, x, A_1, A_2, τ_1, and τ_2 are the same as above.

Voltage dependence of steady-state slow inactivation (s_∞). A 30-s prepulse, a 50-ms step to V_{hold} (to allow recovery from fast inactivation), and then a 4-ms test pulse to +50 mV to record I_{Na}. I_{Na} was normalized to I_{Na} recorded at V_{hold}. In V787K, a 10-s prepulse produced the same results as a 30-s prepulse (data not shown) and a 10-s prepulse is used throughout the study for slow inactivation in V787K. The data from steady-state slow inactivation were fit with a Boltzmann function: $I/I_{max} = (I_1 - I_2)/(1 + \exp((V - V_{1/2})/k)) + I_2$, where $V_{1/2}$ in the midpoint of the curve and k in the slope factor, and I_1 and I_2 are the maximum and minimum values in the fit, respectively.

Recovery from slow inactivation. Voltage was stepped to 0 mV for 30 s (10 s for V787K), stepped to V_{hold} for various times (50 ms to 300 s), then a subsequent 4-ms test pulse to +50 mV. I_{Na} was normalized to I_{Na} obtained after 300 s at V_{hold}. Data were fit with a double-exponential function: $I/I_{max} = I_0 + A_1(1 - \exp(-x/\tau_1)) + A_2(1 - \exp(-x/\tau_2))$, where I_{max}, I_0, x, A_1, A_2, τ_1, and τ_2 are the same as above.

Application of cysteine modification agents

The cysteine modification (MTS) agents methanethiosulfonate ethyltrimethylammonium (MTSET) and MTSEA were obtained from Toronto Research Chemicals (Toronto, Ontario, Canada) and were dissolved in water and kept on ice before dilution in the appropriate solution to the final concentration immediately before use. Extracellular application of the MTS agents was via a gravity-fed perfusion system (≈0.1 ml/min) and the agents were included in the pipette for intracellular application (Yang et al., 1997). Cysteine accessibility during MTS application was determined with a test pulse (+50 mV) every 30 s. For closed-state accessibility the test pulse was from V_{hold} with no prepulse. For fast-inactivated state accessibility there was a 100-ms prepulse (0 mV) and a 10-s interpulse to V_{hold} before each the test pulse. Additional experiments to test for fast-inactivated state accessibility used a train of 100-ms pulses to 0 mV. The train consisted of 100 pulses with a 50-ms interval at V_{hold} between each prepulse and 10-s at V_{hold} before each test pulse (i.e., a total depolarization time of 10 s). For slow-inactivated state accessibility there was a 10-s prepulse (0 mV) and a 10-s interpulse to V_{hold} before each test pulse. Data were collected with an Axopatch 200A amplifier (filtered at 5 kHz) and pCLAMP software (Axon Instruments, Foster City, CA). Curve fits and data analysis were performed with pCLAMP and Origin software (MICROCAL Software, Inc., Northampton, MA). Differences from wild type were considered significant at $p < 0.05$ (Student's t-test). Grouped data are presented as means ± SE.

RESULTS

Activation and fast inactivation differences in V787K and V787C

The h_∞ curve for steady-state fast inactivation was more hyperpolarized and less steep in V787K (−86.6 ± 0.2 mV; $p < 0.001$; $k = 7.7 \pm 0.2$; $p < 0.001$; $n = 7$) and V787C (−87.7 ± 0.3 mV, $p < 0.01$; $k = 7.9 \pm 0.3$; $p < 0.001$; $n = 8$) than in wild type (−81.5 ± 0.1 mV; $k = 5.4 \pm 0.1$; $n = 12$; Fig. 2 *A*). Although steady-state fast inactivation was measured with a standard 100-ms prepulse, the h_∞ curve for V787K probably reflects some channels that have entered the slow inactivation state because of the rapid development of slow inactivation in this mutant (see below). The activation (conductance-voltage) curve was right-shifted and less steep in V787K (−26.5 ± 1.2 mV; $p < 0.05$; $k = 13.4 \pm 1.4$, $p < 0.001$; $n = 7$) and V787C (−20.9 ± 0.9 mV; $p < 0.001$; $k = 11.1 \pm 1.0$; $p < 0.05$; $n = 8$) compared to wild type (−30.0 ± 0.7 mV; $k = 8.9 \pm 0.7$; $n = 12$; Fig. 2 *B*).

V787K recovers from short depolarizations much slower than wild type and V787C

NaChs open and fast-inactivate in response to short depolarizations. Recovery from the fast inactivation state can be assessed by a test pulse following variable recovery times after membrane repolarization to V_{hold}. In the wild type, recovery to initial peak whole-cell sodium current (I_{Na}) from a short depolarization (8 ms at 0 mV) takes ≈30 ms and is best fit with a monoexponential function ($\tau \approx 2$ ms), suggesting recovery from one fast-inactivation state (Fig. 3 *A*; Table 1). In contrast, recovery time to peak I_{Na} in V787K takes 1000 times longer (≈30 s) than wild type. In addition, recovery of V787K is best fit with a double-exponential function ($\tau_1 \approx 1$ ms; $\tau_2 \approx 3$ s), indicating that V787K is recovering from two distinct inactivation states, one of which is much slower than typical fast inactivation (Fig. 3 *A*; Table 1). The difference in recovery pattern is also evident following a 100-ms depolarization (Fig. 3 *B*) where the components of recovery are shifted toward the slower time constant (14−89%; Table 1). These results suggest that V787K is entering a slow inactivation state at a much more rapid rate than wild type. In contrast to V787K, recovery from short depolarizations in V787C is not different from wild type (Fig. 3, *A* and *B*; Table 1).

V787K shows enhanced slow inactivation and V787C is resistant to slow inactivation

Standard slow inactivation protocols were used to study and compare slow inactivation in wild type, V787K, and V787C (O'Reilly et al., 2000). The data from these experiments demonstrate that V787K slow-inactivates much more readily and recovers from slow inactivation more slowly than wild type (Fig. 4, *A* and *B*; Table 1). Fig. 4 *A* shows that the time-dependence of entry into slow inactivation for V787K ($\tau_1 \approx 30$ ms) is 100× faster than wild type ($\tau_1 \approx 3$ s; Table 1). Recovery from slow inactivation at V_{hold} is 10× slower in V787K than wild type ($\tau_1 = 2.7$ vs. 0.3 s, respectively; Fig. 5 *A*; Table 1). The time constant for the

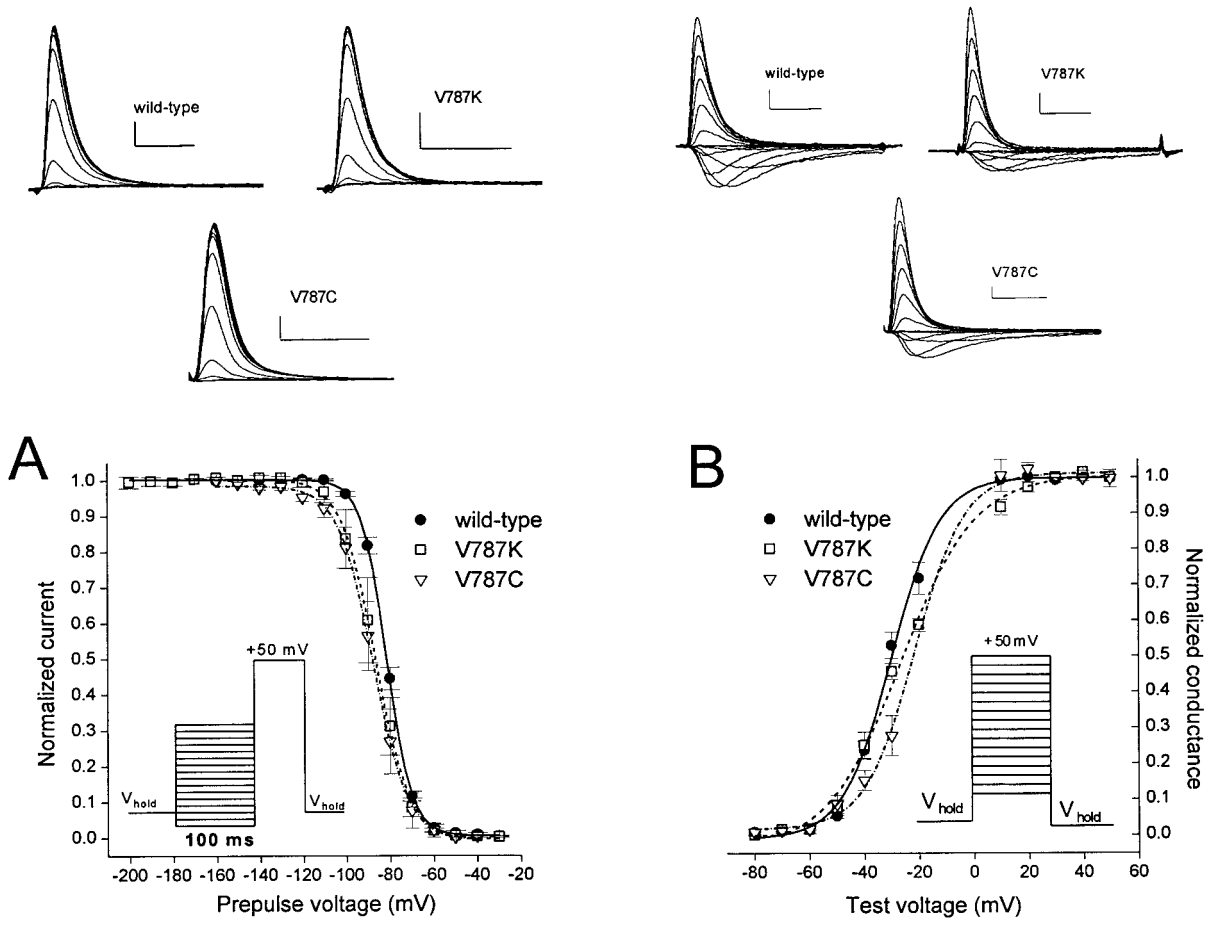

FIGURE 2 The steady-state fast inactivation curve (h_∞) is hyperpolarized and the activation curve is depolarized in V787K and V787C. The data were obtained with the voltage protocol shown in the insets. Mean data ± SE were fit with a Boltzmann function and the $V_{1/2}$ and slope k are given in the text. Representative traces are shown above the graphs. (*A*) Steady-state fast inactivation curves (h_∞) for V787K ($n = 7$), V787C ($n = 8$), and wild type ($n = 12$). (*B*) Activation (conductance-voltage) curves for the same cells as in *A*.

faster component of recovery from slow inactivation in V787K (2.7 s) is similar to the time constants found in recovery from short depolarizations for V787K (3.2 s and 2.8 s; Table 1), supporting the conclusion that V787K is entering the slow inactivation state very rapidly in response to depolarization.

To evaluate the role of a specific amino acid substitution, i.e., lysine (K), at the 787 position, we substituted other amino acids at this position. One of these mutants, V787C (cysteine at position V787), showed a remarkable resistance to slow inactivation compared to wild type, i.e., the opposite phenotype of V787K (Fig. 4, *A* and *B*; Table 1). Compared with wild type and in contrast to V787K, entry into the slow inactivation state was slower in V787C ($\tau_1 \approx 5$ s; Fig. 4 *A*; Table 1) and recovery from slow inactivation was accelerated (Fig. 4 *B*; Table 1).

In addition to differences in development of and recovery from slow inactivation, slow inactivation in V787K occurs at much more hyperpolarized potentials (≈95% inactivation at −100 mV) than wild type (≈2% inactivation at −100 mV) and the $V_{1/2}$ of the s_∞ curve is >50 mV more hyperpolarized in V787K than in wild type (−127.5 vs. −74.1 mV, respectively; Fig. 5 *A*; Table 1). In V787C, slow inactivation was less complete (≈40% slow-inactivated at 0 mV) and the s_∞ curve was shifted to depolarized potentials and was less steep ($V_{1/2} = -50.3$ mV, $k = 16.5$; Fig. 5 *A*; Table 1). These results demonstrate that different amino acid substitutions at the V787 position in $Na_v1.4$ have opposite effects on NaCh slow inactivation.

The difference in slow inactivation among V787K, V787C, and wild type was found at all voltages tested. In Fig. 5 *B*, time constants from single-exponential fits for development of and recovery from slow inactivation in wild type ($n = 3$), V787K ($n = 4$), and V787C ($n = 3$) are plotted versus various test voltages. The data were fit with the equation $\tau = (\beta + \alpha)^{-1}$, where α is the rate for leaving the slow-inactivated state, β is the rate for entering the slow-inactivated state, $\beta(V) = \beta(0)\exp(V/k)$, $\alpha(V) = \alpha(0)\exp(-V/k)$, $\alpha(0)$ and $\beta(0)$ are the rate constants at 0 mV, V is the test voltage, and k is the

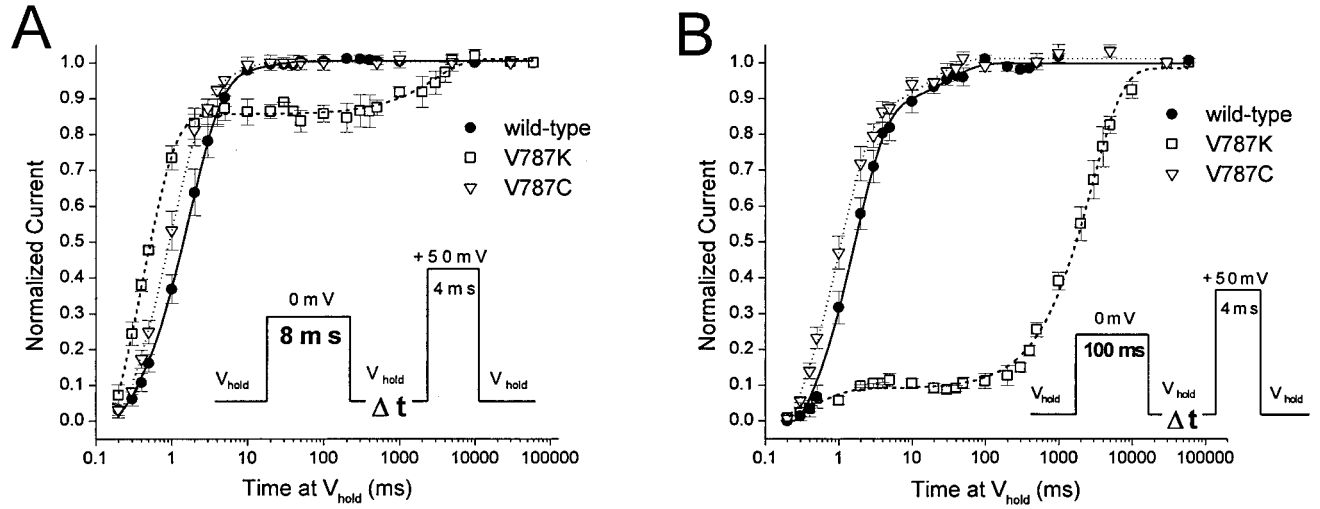

FIGURE 3 V787K recovery from short depolarizations is slower than wild type and V787C. Voltage protocols for recovery from short depolarizations are shown in the insets (also see Materials and Methods). The mean data ± SE were fit with a single exponential (wild type and V787C) or a double exponential (V787K). Time constants and components of the fits are listed in Table 1. The same cells were used for both protocols. (*A*) Recovery to peak I_{Na} from an 8-ms depolarization to 0 mV is slower and best-fit with a double-exponential function in V787K ($n = 5$) suggesting recovery from two inactivation states, fast and slow. (*B*) In wild type ($n = 3$) and V787C ($n = 5$), recovery from a 100-ms depolarization is nearly identical to recovery from an 8-ms pulse (*A*). In V787K, recovery from 100 ms is similar to recovery from the 8-ms pulse except that a larger component of the recovery is from the slow inactivation state (89% vs. 14%).

voltage dependence factor (O'Leary, 1998; O'Reilly et al., 2000). The parameters for the fit are wild type: $\alpha(0) = 1.9 \times 10^{-7}$ ms^{-1}, $\beta(0) = 6.2 \times 10^{-4}$ ms^{-1}, $k_\alpha = 15.1$ mV, $k_\beta = 41.3$ mV; V787K: $\alpha(0) = 1.9 \times 10^{-3}$ ms^{-1}, $\beta(0) = 2.0 \times 10^{-5}$ ms^{-1}, $k_\alpha = 6.7$ mV, $k_\beta = 76.1$ mV; and V787C: $\alpha(0) = 1.2 \times 10^{-8}$ ms^{-1}, $\beta(0) = 1.2 \times 10^{-4}$ ms^{-1}, $k_\alpha = 6.9$ mV, $k_\beta = 74.7$ mV. The data clearly demonstrate that at all voltages tested, V787K slow-inactivates much more rapidly, at more hyperpolarized potentials, and recovers from slow inactivation more slowly, while V787C is resistant to slow inactivation, compared with wild type.

TABLE 1 Short depolarizations and slow inactivation in wild-type and V787 mutants

Channel	Recovery from 8 ms at 0 mV; τ (ms), component (%) [n]	Recovery from 100 ms at 0 mV; τ (ms), component (%) [n]	Recovery from slow inactivation; τ (ms), component (%) [n]	Entry into slow inactivation; τ (ms), component (%) [n]	Steady-state slow inactivation (s_∞); $V_{1/2}$ (mV), slope k [n]
Wild type	1.7 ± 0.1 [3]	1.7 ± 0.1 [3]	261 ± 27 (59) 3789 ± 490 (34) [7]	2752 ± 118 (75%) 26948 ± 7957 (14%) [8]	−74.1 ± 1.1 9.9 ± 0.9 [8]
V787K	0.7 ± 0.1* (86) 3171 ± 1580 (14) [5]	0.5 ± 0.3* (12) 2822 ± 106 (89) [5]	2667 ± 547* (70) 18481 ± 1103* (25) [6]	30.3 ± 7.0* (85) 104.8 ± 72.0* (14) [6]	−127.5 ± 1.5* 15.9 ± 1.3* [6]
V787C	1.6 ± 0.4 [5]	1.7 ± 0.1 [5]	178 ± 50† (32) 2161 ± 613† (13) [4]	5096 ± 2616* (33) 16474 ± 3624* (8) [7]	−50.3 ± 3.0* 16.5 ± 2.6* [4]
V787A	1.6 ± 0.7 [4]	1.6 ± 0.2 [4]	122 ± 31* (66) 3547 ± 1578 (13) [4]	3902 ± 381* (51) 38419 ± 2014* (14) [7]	−49.9 ± 1.6* 14.5 ± 1.4* [7]
V787D	1.3 ± 0.1 [5]	1.9 ± 0.1 [5]	346 ± 67 (45) 12332 ± 2654‡ (35) [3]	1604 ± 221 (58) 24712 ± 8423 (13) [8]	−57.9 ± 1.8* 10.6 ± 1.7 [5]

The data presented in the first four columns are time constants ± SEM (ms) and components (%) from single- or double-exponential fits of the mean data for recovery (at V_{hold}) of peak Na^+ current (I_{Na}) following an 8- or 100-ms depolarization to 0 mV, recovery of I_{Na} from slow inactivation (10 or 30 s at 0 mV), and entry into slow inactivation at 0 mV, respectively. See text for additional details. The data presented in the last column describe steady-state slow inactivation (s_∞). The mean data for the s_∞ curve were fit with a Boltzmann function and the $V_{1/2}$ (mV) and slope factor k ± SEM are presented. The voltage protocols are described in Materials and Methods. [n] = Number of cells.
*$p < 0.001$, † = $p < 0.05$, ‡ = $p < 0.01$ compared with wild type.

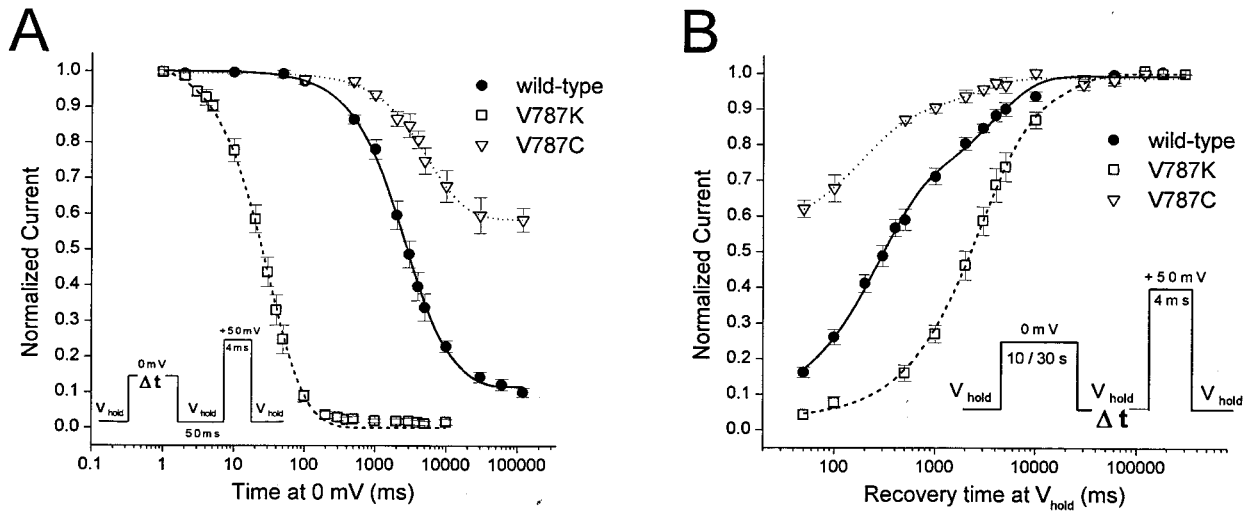

FIGURE 4 V787K slow-inactivates more readily and V787C is relatively resistant to slow inactivation. Data were collected with the voltage protocols shown in the insets (also see Materials and Methods). Mean data ± SEM were fit with a double-exponential function. Time constants and components of the fits are listed in Table 1. (*A*) V787K ($n = 6$) enters the slow inactivation state 100× faster ($\tau_1 \approx 30$ ms) than wild type ($\tau_1 \approx 3000$ ms; $n = 8$) and 100% of the current in V787K slow-inactivates by 1 s, whereas only ≈85% of wild type I_{Na} slow-inactivates even after 120 s of depolarization. V787C ($n = 7$) slow-inactivates with slower time constants and less completely than wild type or V787K. (*B*) Compared to wild type ($n = 7$), recovery from slow inactivation is slower in V787K ($n = 6$) and faster in V787C ($n = 4$).

MTSEA modification of V787C in the slow inactivation state

We used the cysteine accessibility method in V787C to see whether we could determine the molecular location of the 787 residue during slow inactivation gating (Akabas et al., 1992; Yellen, 1998; Vedantham and Cannon, 2000). We used a test pulse (+50 mV) every 30 s to measure I_{Na} during continuous exposure to cysteine-modifying agents. Initial

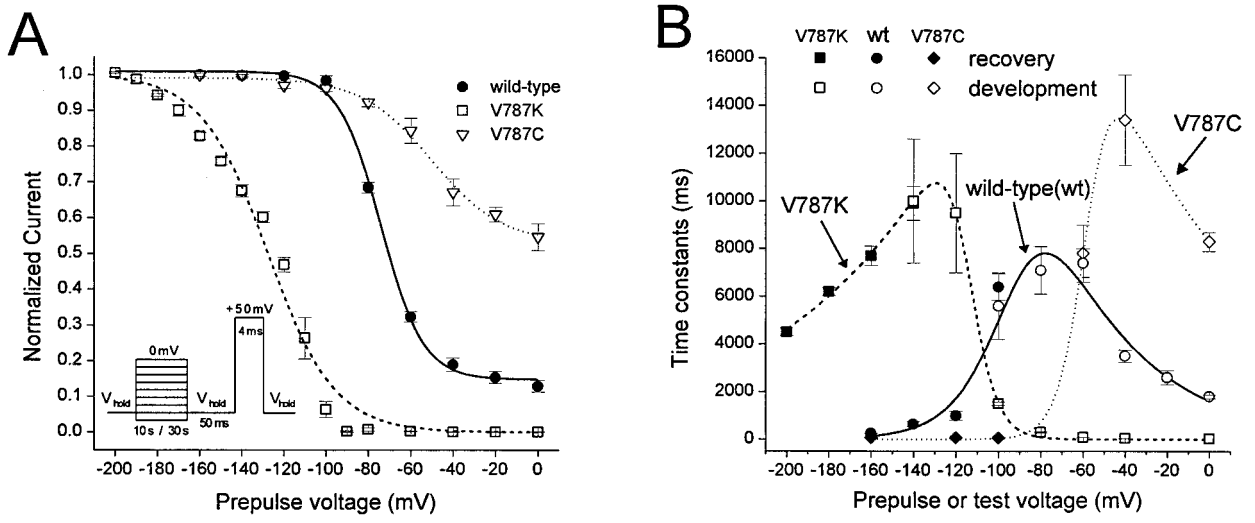

FIGURE 5 V787K slow-inactivates at more hyperpolarized potentials while V787C slow-inactivates at more depolarized potentials than wild type. (*A*) Data were collected with the voltage protocol shown in the inset (also see Materials and Methods). Mean data ± SE were fit with a Boltzmann function and $V_{1/2}$ and slope k from the fits are given in Table 1. The s_∞ curve is hyperpolarized by >50 mV in V787K ($n = 6$) compared to wild type ($n = 8$). Also note that slow inactivation in V787K is complete by ≈−90 mV, whereas wild type shows little inactivation at this voltage. Voltage dependence of slow inactivation (s_∞ curve) in V787C ($n = 4$) is shifted in the depolarized direction ($V_{1/2} \approx -50$ mV). In addition, V787C exhibits much less slow inactivation than wild type at all voltages above −80 mV. (*B*) The graph shows time constants from single-exponential fits of mean data for development of (*open symbols*) and recovery from (*filled symbols*) slow inactivation plotted versus the voltages on the abscissa. The data were fit with the equation $\tau = (\beta + \alpha)^{-1}$, where α is the rate for leaving the slow-inactivated state, β is the rate for entering the slow-inactivated state, $\beta(V) = \beta(0)\exp(V/k)$, $\alpha(V) = \alpha(0)\exp(-V/k)$, $\alpha(0)$ and $\beta(0)$ are the rate constants at 0 mV, V is the test voltage, and k is the voltage dependence factor. The rate constants and slopes are given in the text. Compared with wild type (*solid line*; $n = 3$), V787K (*dashed line*; $n = 4$) enters slow inactivation faster and recovers slower and V787C (*dotted line*; $n = 3$) enters slow inactivation slower and recovers faster at all test voltages.

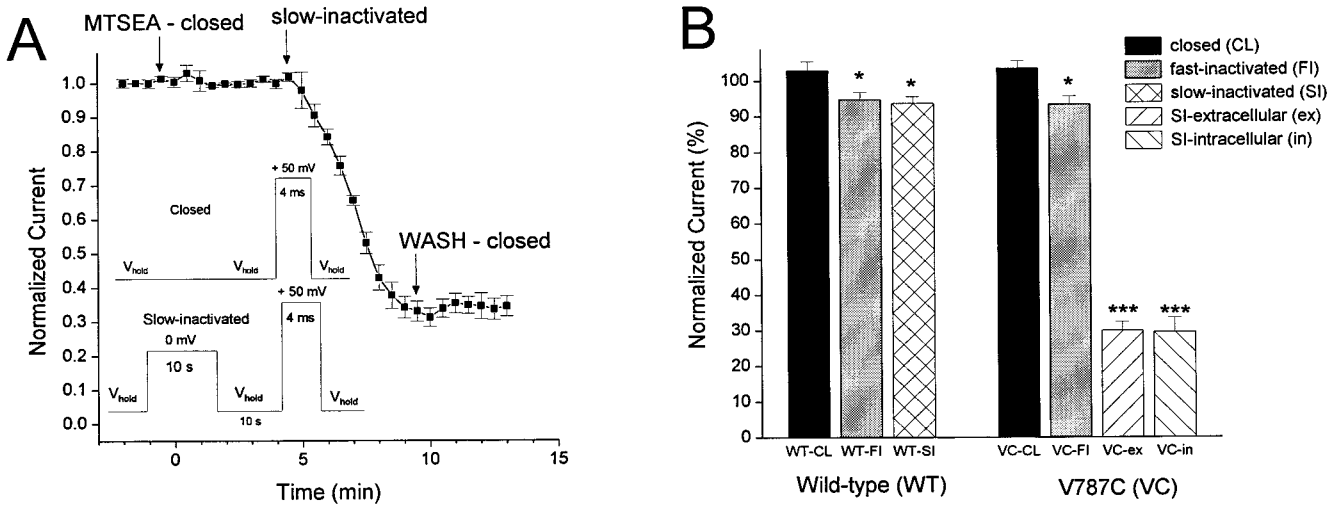

FIGURE 6 MTSEA reacts with V787C in the slow-inactivated state. (*A*) Cells expressing V787C ($n = 4$) were continuously exposed (extracellular) to 1.5 mM MTSEA starting at time 0. Peak available I_{Na} was recorded every 30 s with a test pulse to +50 mV. For the closed state, the test pulse was from V_{hold} with no prepulse; the slow-inactivated state was produced with a 10-s prepulse before each test pulse (*insets*). Also see text and Materials and Methods for further description of the protocols. MTSEA reduced I_{Na} only when the test pulse was preceded with a 10-s prepulse to 0 mV, i.e., when the channels were slow-inactivated. The MTSEA-induced reduction in I_{Na} was irreversible at V_{hold} of −160 mV or −200 mV. (*B*) Grouped data for wild type and V787C exposed to 1.5 mM MTSEA for 5 min in the closed state (no prepulse), fast-inactivated state (100-ms prepulse or 100-ms × 100 train), and the slow-inactivated state (10-s prepulse). In wild type, 5-min exposure to MTSEA had no effect in the closed state and only modest effects in the fast- or slow-inactivated states. In V787C, MTSEA had no effect in the closed state and only a modest effect in the fast-inactivated state. However, in the slow-inactivated state there was a large and prominent reduction in I_{Na} during exposure to MTSEA. Means and SEM are given in the text, as are the number of cells for each group. WT, wild type; VC, V787C; CL, closed state; FI, fast-inactivated state; SI, slow-inactivated state; ex, extracellular application of MTSEA; in, intracellular application of MTSEA. * $p < 0.05$; *** $p < 0.001$ compared with wild-type closed state.

experiments in V787C with MTSET (up to 1 mM) produced no significant changes in I_{Na} either from the intracellular ($n = 8$) or the extracellular side ($n = 6$) of the membrane when the channels were closed, open, fast-inactivated, or slow-inactivated (data not shown). Application of MTSEA at 1.5 mM on the extracellular or intracellular side of the membrane had little effect in V787C when the channels were closed, i.e., with no prepulse before the test pulse (103.6 ± 2.0% of initial peak I_{Na} after 5-min exposure; $n = 20$; Fig. 6, *A* and *B*). However, when the membrane was depolarized (0 mV) for 10 s before each test pulse, i.e., producing slow inactivation, there was a prominent reduction in peak I_{Na} over the course of several minutes (Fig. 6, *A* and *B*). This effect was found with extracellular (30.0 ± 2.4%; $n = 18$) and intracellular (29.6 ± 4.0%; $n = 3$) application of MTSEA (Fig. 6, *A* and *B*). In addition, peak I_{Na} did not recover from the MTSEA modification as monitored by test pulses from V_{hold} of −160 mV or −200 mV (Fig. 6 *A*).

The MTSEA-induced reduction in I_{Na} appears to be unique to the slow inactivation state in V787C because experiments using short prepulses (to produce fast inactivation) did not result in the same reduction in peak I_{Na} as the slow-inactivation protocol. For example, fast-inactivation protocols using a 100-ms prepulse to 0 mV or a prepulse depolarization train (0 mV, 100-ms duration, 50-ms intervals, 100 pulses) before each test pulse resulted in only a modest reduction in I_{Na} during 5 min of MTSEA exposure (93.5 ± 2.2%; extra or intracellular; $n = 17$; Fig. 6 *B*). The rapid pulses in the latter protocol also suggest that MTSEA does not react readily with channels that are in the open state.

In wild type, MTSEA application had no effect with the closed-state protocol using no prepulse (102.9 ± 2.5%; extra or intracellular; $n = 9$; Fig. 6 *B*) and caused only a modest reduction of I_{Na} with the slow-inactivation 10-s prepulse protocol (93.8 ± 1.8%; extra or intracellular; $n = 10$; Fig. 6 *B*) or with the fast-inactivation 100-ms prepulse or the 100-ms train prepulse protocols (94.8 ± 2.0%; extra or intracellular; $n = 13$; Fig. 6 *B*). These results indicate that MTSEA-induced reduction in I_{Na} is specific to V787C and that the 787C residue is accessible to MTSEA only when the channel is in the slow-inactivated state. This also suggests that there is a molecular conformational change at or near the V787 position in $Na_v1.4$ that occurs in response to prolonged depolarization that produces slow inactivation.

Other amino acid substitutions at V787

We also made several other amino acid substitutions at position V787 to see whether different substitutions would provide additional molecular insight into the mechanisms of slow inactivation. Mutants with arginine (V787R) or ty-

rosine (V787Y) substituted at V787 expressed little or no I_{Na} (<1.0 nA at the test pulse of +50 mV from V_{hold} of −200 mV). Alanine (V787A) and aspartate (V787D) substitutions expressed adequate I_{Na} for study and showed differences from wild type in activation and fast inactivation that were similar to V787K and V787C, e.g., see Fig. 2, *A* and *B* (data not shown). The slow inactivation phenotype in V787A and V787D was similar to wild type or intermediate between wild type and V787C, i.e., a relative resistance to slow inactivation (Table 1). For example, V787A exhibits a slow inactivation phenotype similar to V787C, but is not as dramatically different from wild type as V787C (Table 1). These results demonstrate that the lysine substitution in V787K has a unique effect on slow inactivation that may be due to the positive charge of the side chain, while other amino acid substitutions probably disrupt critical molecular conformation necessary for the normal slow inactivation gating process, possibly as a result of subtle changes in the three-dimensional structure of the amino acid side chain at V787.

DISCUSSION

In this study we have characterized activation and inactivation in rat skeletal muscle NaCh μ1 ($Na_v1.4$) mutants that have a single amino acid substitution at position V787 in domain 2, segment 6 (D2-S6). In particular, we studied the effects of these substitutions on slow inactivation phenotype. Our results show that one mutant, V787K, rapidly enters the slow inactivation state and that another mutant, V787C, is relatively resistant to entry into slow inactivation, i.e., different amino acid substitutions at the same position have opposite effects on slow inactivation. We propose that a depolarization-induced conformational change alters the relative position of the 787 residue. We hypothesize that development of slow inactivation is promoted and stabilized by the positive charge of lysine (K), while the slow inactivation conformational state is destabilized by amino acid substitutions (e.g., cysteine, C) that create subtle changes in the three-dimensional structure of the 787 residue.

Activation and fast inactivation in wild-type and V787 mutants

Compared with wild type, the steady-state fast inactivation (h_∞) curve is more hyperpolarized, the activation (conductance-voltage) curve is shifted in the positive direction, and both curves are less steep in V787K, V787C, and the other V787 mutants studied. Changes in these parameters are quite common with point mutations in voltage-gated channels. Even amino acid substitutions that would be considered relatively benign, e.g., alanine, can have large effects on activation and fast inactivation (Yarov-Yarovoy et al., 2001). These effects probably reflect disruption of molecular cooperativity within the channel during fast voltage gating. For example, disruption of cooperative molecular interactions can explain shifts in midpoints and reduction in slopes of activation curves for voltage-gated ion channels (Tytgat and Hess, 1992).

The differences in activation and fast inactivation may or may not be the direct result of these specific amino acid substitutions. It may be that the absence of the native valine at 787 disrupts normal molecular movement and cooperativity during fast voltage gating, so that any amino acid substitution at 787 would have disruptive effects on fast inactivation and activation.

Recovery from short depolarizations suggest rapid inactivation in V787K

Recovery to peak I_{Na} following relatively short depolarizations of 8 or 100 ms is much slower in V787K than in wild-type and the other V787 mutants. In addition, recovery in V787K is best fit with a double-exponential function (in contrast to a single-exponential fit for wild-type and the other V787 mutants), which suggests that V787K is recovering from two distinct inactivation states. We believe that the recovery pattern in V787K represents recovery from the typical fast inactivation state and a slow inactivation state similar to those found in wild type. That is, V787K and wild type are recovering from the same inactivation states (fast and slow), but V787K enters the slow inactivation state faster than wild type. Hence, wild type exhibits a single-exponential recovery pattern because there is no slow inactivation in wild type in response to 8 or 100 ms depolarizations, whereas V787K fast- and slow-inactivate during these relatively brief depolarizations. This conclusion is supported by data from our slow inactivation protocols showing that V787K rapidly enters the slow inactivation state compared to wild type (see below). It should also be noted that the fast component of recovery from short depolarizations in V787K has a faster time constant than in wild type (0.5–0.7 vs. 1.7 ms). This may be due to a direct effect of the lysine substitution on fast inactivation gating or it could be due to an alteration of molecular coupling between slow and fast inactivation (Featherstone et al., 1996).

V787K enters the slow inactivation state more readily and recovers from slow inactivation more slowly than wild type

Standard slow inactivation protocols demonstrate that V787K enters an inactivation state(s) very rapidly and at remarkably hyperpolarized potentials compared with wild type. We believe that these results represent accelerated entry into the typical slow inactivation state(s) found in wild type. We base this conclusion on the double-exponential fit of the data from our double-pulse inactivation protocols.

For example, the similar time constants ($\tau \approx 3$ s) for recovery from short (8 or 100 ms) or longer (10 s) depolarizations suggest that V787K has rapidly entered the same slow inactivation state in response to short or prolonged depolarization. Voltage protocols that measure the time-dependence of development of slow inactivation show that entry into slow inactivation is 100× faster in V787K than in wild type. Both V787K and wild type enter a second slow inactivation state and again V787K enters this state more rapidly (≈100×) than wild type. Although V787K slow-inactivates very rapidly, the components of the double-exponential fits of the data are similar between wild type and V787K, supporting our conclusion that V787K is entering slow inactivation states that are found in the wild-type channel, but at more rapid rates. We cannot absolutely rule out the possibility that these inactivation state(s) are unique to V787K. For example, a lysine substitution in D4-S6 (Y1586K) produces a distinct and novel "atypical" inactivation state in $Na_v1.4$ (O'Reilly et al., 2000). However, in the present study the absence of any extra components in the exponential fits of the data suggest that V787K enters the same inactivation states as wild type. The rapid development of slow inactivation in V787K could result from a depolarization-induced conformational change of D2-S6 that alters the relative position of residue 787. This dynamic change in the relative position of 787K could result in an electrostatic interaction with a molecular substrate (e.g., arginine, glutamate, π-electrons of phenylalanine) that results in an increase in the stability of the slow inactivation state.

The slowed recovery and the remarkably hyperpolarized s_∞ curve (>50 mV) of slow inactivation in V787K suggest that the slow inactivation state in this mutant is a very stable molecular conformation. This conclusion is supported by the data showing that entry into slow inactivation is very rapid and recovery from slow inactivation is greatly slowed at all voltages tested. We also believe that the effects on slow inactivation of the lysine substitution at V787 may be unique to this particular position in D2-S6 because substitution of lysine at other positions in D2-S6 (N784K, L785K, L788K) produce no prominent effects on slow inactivation (Wang et al., 2001). In addition, charge per se does not appear to be responsible because V787D (a negatively charged substitution) did not show the dramatic slow inactivation phenotype found in V787K.

Cysteine substitution in V787C produces opposite effects on slow inactivation

In contrast to V787K, we found that the mutant V787C (and to varying degrees, other substitutions) showed the opposite effect of V787K, i.e., a resistance to slow inactivation. The relative resistance to slow inactivation in V787C may be due to the change in the size or structure of the side chain at 787 from the branched, three-carbon side chain of the native valine to the short carbon-sulfur side chain of cysteine. For example, part of the slow inactivation gate(s) may be dependent on an intramolecular association that requires the specific side chain of valine. Hence, a smaller or less "bulky" side chain may destabilize the slow inactivation state, which would result in a relative resistance to development of slow inactivation in V787C. This result also demonstrates that amino acid substitutions such as cysteine, which may be considered relatively benign, can potentially have rather prominent effects on the function of voltage-gated channels and that results from experiments using cysteine substitutions should be interpreted with caution.

MTSEA modification of V787C in the slow inactivation state

We used the cysteine accessibility method to explore the possibility of molecular movement at or near the 787 residue during slow inactivation gating (Akabas et al., 1992; Yang et al., 1997; Yellen, 1998; Vedantham and Cannon, 2000). Experiments with MTSET in V787C (intracellular or extracellular) produced no significant change in I_{Na}, and hence were inconclusive. However, because MTSET is hydrophilic and does not readily enter or cross the membrane, these results may indicate that 787C is not located in a hydrophilic environment (e.g., not facing the pore) or that MTSET may be too large to reach the 787C residue. Another possibility is that MTSET reacts with 787C but produces no measurable change in I_{Na}. Experiments with MTSEA, which is smaller than MTSET and can enter the membrane (Holmgren et al., 1996), showed that the 787C residue is accessible to MTSEA when the channel is in the slow-inactivated state, but that it is not accessible when the channel is in the closed, open, or fast-inactivated state. Support for this conclusion comes from the different inactivation protocols that we used. For example, the slow-inactivation protocol had a 10-s depolarization prepulse before the test pulse, which is sufficient to produce slow inactivation in V787C. Application of MTSEA to V787C during this slow-inactivation protocol resulted in a prominent reduction in I_{Na}. In contrast, the fast-inactivation protocol with the 100-ms depolarization train (100 ms × 100 pulses) resulted in only modest effects on I_{Na} during MTSEA exposure in V787C. This difference was evident even though the slow-inactivation protocol and the fast-inactivation protocol both used 10-s depolarization. However, the fast-inactivation protocol resulted in the channels being in the fast-inactivated state, not the slow-inactivated state, because 100-ms depolarization produces little if any slow inactivation and the channels were allowed to recover from fast inactivation (V_{hold} for 50 ms) between each 100-ms depolarization prepulse. The rapid prepulses of this protocol also suggest that 787C is not readily accessible to MTSEA during the open state, and test pulses from V_{hold} with no prepulse demonstrated that MTSEA does not react with

787C in the closed state. One interpretation of these results would be that the 787C residue is "buried" within the protein when the channel is in the open, closed, and fast-inactivated state and only becomes "accessible" to react with MTSEA in the slow inactivation state. We cannot conclude precisely from these results whether MTSEA reaches the 787C residue via a hydrophilic (i.e., the pore) or a hydrophobic environment (i.e., the membrane) because MTSEA can reach the site through either pathway. However, this result does demonstrate that there is a molecular rearrangement at or near the 787 position associated with the slow inactivation state that alters the relative position of this residue.

An intriguing interpretation of the MTSEA-induced reduction of I_{Na} in V787C is that covalent modification of 787C by MTSEA would result in a molecular side chain that resembles the side chain of lysine. Therefore, MTSEA-modified V787C may mimic the enhanced slow inactivation seen in V787K by adding a positive charge at this position. However, I_{Na} did not recover to initial values when the membrane was held at V_{hold} of -200 mV (up to 30 s), a recovery which would be expected if MTSEA-modified V787C was similar to V787K. Hence, it appears that MTSEA modification of V787C results in a nonconducting state that is different from the enhanced slow inactivation found in V787K. Indeed, it may be that MTSEA modification of V787C more closely resembles arginine substitution at V787, i.e., V787R, a mutant that failed to express Na^+ current.

Other amino acid substitutions at V787

We substituted several other amino acid residues at the V787 position. Of these, half failed to express adequate current for study. We usually define adequate current as a peak Na^+ current of at least 1.0 nA with a test pulse of $+50$ mV from V_{hold}, which avoids recording and analyzing potential background Na^+ currents in HEK cells (Cummins et al., 1999). In the mutants that did express current we observed slow inactivation phenotypes that were similar to wild type or intermediate between wild type and V787C. Hence, we conclude that subtle changes in the three-dimensional structure of the side chain at V787 in these mutants disrupts a critical molecular conformation that is necessary for normal slow-inactivation gating in $Na_v1.4$.

Potential molecular mechanisms of NaCh slow inactivation

Depolarization-induced conformational changes in voltage-gated channels, including NaChs, is well-established (Yellen, 1998). In particular, depolarization is thought to produce a rotation around a central bundle crossing of the S6 segments in the inner pore region of voltage-gated K^+ channels, which suggests that this region is an important component of voltage gating (Holmgren et al., 1998). Assuming a common evolutionary pathway for voltage-gated channels (Hille, 1989), we would expect to find a similar molecular mechanism for voltage gating in NaChs. Indeed, a recent study in $Na_v1.4$ has shown that the V1583 residue in D4-S6 of the inner pore moves in response to depolarization that produces slow inactivation, thereby suggesting that this region also plays a role in voltage gating of NaChs (Vedantham and Cannon, 2000). Our data from the current study indicate that V787 in D2-S6 also moves during slow-inactivation gating. However, an interesting comparison between V1583 and V787 is that, during slow-inactivation gating, the V1583 residue becomes inaccessible to MTSEA (Vedantham and Cannon, 2000), while the V787 residue becomes accessible to MTSEA (this study), suggesting a dynamic molecular rearrangement of this region of $Na_v1.4$ in response to prolonged depolarization that produces slow inactivation. Also, this area of $Na_v1.4$ has previously been implicated in slow inactivation in a study from our laboratory that showed that a mutation in D1-S6 (N434A) accelerates slow inactivation (Wang and Wang, 1997). Of interest is that all of these S6 positions (V1583, V787, and N434) are located at approximately the same level of the inner pore of $Na_v1.4$ (Lipkind and Fozzard, 2000). These results suggest that the S6 segments of the inner pore play an important role in NaCh slow inactivation and that the region where N434, V787, and V1583 converge may be a molecular determinant for part of the slow-inactivation gate.

Additional support for this model of S6 involvement in NaCh inactivation comes from studies with batrachotoxin (BTX). BTX is an alkaloid neurotoxin that binds to NaChs and dramatically alters NaCh gating, shifting activation in the hyperpolarizing direction and essentially eliminating fast and slow inactivation (Khodorov, 1985). Recent studies have shown that BTX binds to the S6 segments of all four domains of NaChs (Wang and Wang, 1998, 1999; Wang et al., 2000, 2001). Specifically, BTX binds to residues (I433, N434, L437, N784, L788, S1276, L1280, F1579, N1584) in the region where N434, V787, and V1583 converge. These results suggest that BTX-induced effects on voltage gating in NaChs may be due to disruption of specific molecular determinants of activation and/or inactivation gate(s) in the inner pore formed by all four of the S6 segments.

We propose a model for NaCh slow inactivation in which the S6 segments play an important molecular role. This model predicts that the inner parts of the S6 segments near the N434, V787, and V1583 positions assume a unique molecular conformation during prolonged depolarizations that stabilizes the inner pore in a nonconducting, slow inactivation state. Although we believe that the S6 segments play a prominent role in NaCh slow inactivation, we appreciate the complex molecular nature of this process and do not assume that the S6 segments are the only molecular determinants of NaCh slow inactivation. For example, mu-

tations in other parts of NaChs can have various effects on slow inactivation (Cummins and Sigworth, 1996; Hayward et al., 1997, 1999; Vilin et al., 1999; Struyk et al., 2000; Bendahhou et al., 2000).

In conclusion, our results suggest that the V787 position plays an important role in NaCh slow inactivation. We hypothesize that prolonged depolarization produces a change in the relative position of the positively charged residue in V787K that results in an intramolecular electrostatic interaction that accelerates and stabilizes the slow-inactivation state. The opposite effect is observed when different residues are substituted at the V787 position (e.g., V787C) that may be due to a disruption of a highly specific intramolecular interaction required for normal slow-inactivation gating in $Na_v1.4$.

This work was supported by National Institutes of Health Grants GM35401 and GM 49090. J.O.R. is supported by a National Research Service Award from the National Heart, Lung, and Blood Institute of the National Institutes of Health.

REFERENCES

Akabas, M. H., D. A. Stauffer, M. Xu, and A. Karlin. 1992. Acetylcholine receptor channel structure probed in cysteine-substitution mutants. *Science.* 258:307–310.

Aldrich, R. W., D. P. Corey, and C. F. Stevens. 1983. A reinterpretation of mammalian sodium channel gating based on single channel recording. *Nature.* 306:436–441.

Armstrong, C. M., F. Bezanilla, and E. Rojas. 1973. Destruction of sodium conductance inactivation in squid axons perfused with pronase. *J. Gen. Physiol.* 62:375–391.

Bendahhou, S., T. R. Cummins, A. F. Hahn, S. Langlois, S. G. Waxman, and L. J. Ptacek. 2000. A double mutation in families with periodic paralysis defines new aspects of sodium channel slow inactivation. *J. Clin. Invest.* 106:431–438.

Cannon, S. C., and S. M. Strittmatter. 1993. Functional expression of sodium channel mutations identified in families with periodic paralysis. *Neuron.* 10:317–326.

Cota, G., and C. M. Armstrong. 1989. Sodium channel gating in clonal pituitary cells. The inactivation step is not voltage dependent. *J. Gen. Physiol.* 94:213–232.

Cummins, T. R., S. D. Dib-Hajj, J. A. Black, A. N. Akopian, J. N. Wood, and S. G. Waxman. 1999. A novel persistent tetrodotoxin-resistant sodium current in SNS-null and wild-type small primary sensory neurons. *J. Neurosci.* 19:RC43.

Cummins, T. R., and F. J. Sigworth. 1996. Impaired slow inactivation in mutant sodium channels. *Biophys. J.* 71:227–236.

Featherstone, D. E., J. E. Richmond, and P. C. Ruben. 1996. Interaction between fast and slow inactivation in Skm1 sodium channels. *Biophys. J.* 71:3098–3109.

Gellens, M. E., A. L. J. George, L.-Q. Chen, M. Chahine, R. Horn, R. L. Barchi, and R. G. Kallen. 1992. Primary structure and functional expression of the human cardiac tetrodotoxin-insensitive voltage-dependent sodium channel. *Proc. Natl. Acad. Sci. U.S.A.* 89:554–558.

Graham, F. L., and A. J. Eb. 1973. A new technique for the assay of infectivity of human adenovirus 5 DNA. *Virology.* 52:456–467.

Hamill, O. P., A. Marty, E. Neher, B. Sakmann, and F. J. Sigworth. 1981. Improved patch-clamp techniques for high-resolution current recording from cells and cell-free membrane patches. *Pflugers Arch.* 391:85–100.

Hayward, L. J., R. H. J. Brown, and S. C. Cannon. 1997. Slow inactivation differs among mutant Na channels associated with myotonia and periodic paralysis. *Biophys. J.* 72:1204–1219.

Hayward, L. J., G. M. Sandoval, and S. C. Cannon. 1999. Defective slow inactivation of sodium channels contributes to familial periodic paralysis. *Neurology.* 52:1447–1453.

Heinemann, S. H., H. Terlau, W. Stuhmer, K. Imoto, and S. Numa. 1992. Calcium channel characteristics conferred on the sodium channel by single mutations. *Nature.* 356:441–443.

Hille, B. 1989. The Sharpey-Schafer lecture. Ionic channels: evolutionary origins and modern roles. *Q. J. Exp. Physiol.* 74:785–804.

Hille, B. 1992. Ionic Channels of Excitable Membranes. Sinauer Associates, Sunderland, MA.

Hodgkin, A. L., and A. E. Huxley. 1952:A quantitative description of membrane current and its application to conduction and excitation in nerve. *J. Physiol. (Lond.).* 117:500–544.

Holmgren, M., Y. Liu, Y. Xu, and G. Yellen. 1996. On the use of thiol-modifying agents to determine channel topology. *Neuropharmacology.* 35:797–804.

Holmgren, M., K. S. Shin, and G. Yellen. 1998. The activation gate of a voltage-gated K+ channel can be trapped in the open state by an intersubunit metal bridge. *Neuron.* 21:617–621.

Khodorov, B. I. 1985. Batrachotoxin as a tool to study voltage-sensitive sodium channels of excitable membranes. *Prog. Biophys. Mol. Biol.* 45:57–148.

Lipkind, G. M., and H. A. Fozzard. 2000. KcsA crystal structure as framework for a molecular model of the Na(+) channel pore. *Biochemistry.* 39:8161–8170.

McPhee, J. C., D. S. Ragsdale, T. Scheuer, and W. A. Catterall. 1998. A critical role for the S4–S5 intracellular loop in domain IV of the sodium channel α-subunit in fast inactivation. *J. Biol. Chem.* 273:1121–1129.

Noda, M., T. Ikeda, T. Kayano, H. Suzuki, H. Takeshima, M. Kurasaki, H. Takahashi, and S. Numa. 1986. Existence of distinct sodium channel messenger RNAs in rat brain. *Nature.* 320:188–192.

Noda, M., S. Shimizu, T. Tanabe, T. Takai, T. Kayano, T. Ikeda, H. Takahashi, H. Nakayama, Y. Kanaoka, and N. Minamino. 1984. Primary structure of *Electrophorus electricus* sodium channel deduced from cDNA sequence. *Nature.* 312:121–127.

O'Leary, M. E. 1998. Characterization of the isoform-specific differences in the gating of neuronal and muscle sodium channels. *Can. J. Physiol. Pharmacol.* 76:1041–1050.

O'Reilly, J. P., S.-Y. Wang, R. G. Kallen, and G. K. Wang. 1999. Comparison of slow inactivation in human heart and rat skeletal muscle Na channel chimeras. *J. Physiol. (Lond.).* 515.1:61–73.

O'Reilly, J. P., S.-Y. Wang, and G. K. Wang. 2000. A point mutation in domain 4-segment 6 of the skeletal muscle sodium channel produces an atypical inactivation state. *Biophys. J.* 78:773–784.

Patton, D. E., J. W. West, W. A. Catterall, and A. L. Goldin. 1992. Amino acid residues required for fast Na^+-channel inactivation: charge neutralizations and deletions in the III-IV linker. *Proc. Natl. Acad. Sci. U.S.A.* 89:10905–10909.

Rudy, B. 1978. Slow inactivation of the sodium conductance in squid giant axons. Pronase resistance. *J. Physiol. (Lond.).* 283:1–21.

Ruff, R. L., L. Simoncini, and W. Stuhmer. 1988. Slow sodium channel inactivation in mammalian muscle: a possible role in regulating excitability. *Muscle Nerve.* 11:502–510.

Sawczuk, A., R. K. Powers, and M. D. Binder. 1995. Spike frequency adaptation studied in hypoglossal motoneurons of the rat. *J. Neurophysiol.* 73:1799–1810.

Smith, M. R., and A. L. Goldin. 1997. Interaction between the sodium channel inactivation linker and domain III S4–S5. *Biophys. J.* 73: 1885–1895.

Struyk, A. F., K. A. Scoggan, D. E. Bulman, and S. C. Cannon. 2000. The human skeletal muscle Na channel mutation R669H associated with hypokalemic periodic paralysis enhances slow inactivation. *J. Neurosci.* 20:8610–8617.

Stuhmer, W., F. Conti, H. Suzuki, X. D. Wang, M. Noda, N. Yahagi, H. Kubo, and S. Numa. 1989. Structural parts involved in activation and inactivation of the sodium channel. *Nature.* 339:597–603.

Takahashi, M. P., and S. C. Cannon. 1999. Enhanced slow inactivation by V445M: a sodium channel mutation associated with myotonia. *Biophys. J.* 76:861–868.

Trimmer, J. S., S. S. Cooperman, S. A. Tomiko, J. Y. Zhou, S. M. Crean, M. B. Boyle, R. G. Kallen, Z. H. Sheng, R. L. Barchi, and F. J. Sigworth. 1989. Primary structure and functional expression of a mammalian skeletal muscle sodium channel. *Neuron.* 3:33–49.

Tytgat, J., and P. Hess. 1992. Evidence for cooperative interactions in potassium channel gating. *Nature.* 359:420–423.

Ukomadu, C., J. Zhou, F. J. Sigworth, and W. S. Agnew. 1992. μI Na^+ channels expressed transiently in human embryonic kidney cells: biochemical and biophysical properties. *Neuron.* 8:663–676.

Vedantham, V., and S. C. Cannon. 2000. Rapid and slow voltage-dependent conformational changes in segment IVS6 of voltage-gated Na(+) channels. *Biophys. J.* 78:2943–2958.

Vilin, Y. Y., N. Makita, A. L. J. George, and P. C. Ruben. 1999. Structural determinants of slow inactivation in human cardiac and skeletal muscle sodium channels. *Biophys. J.* 77:1384–1393.

Wang, S.-Y., M. Barile, and G. K. Wang. 2001. Disparate role of Na(+) channel D2–S6 residues in batrachotoxin and local anesthetic action. *Mol. Pharmacol.* 59:1100–1107.

Wang, S.-Y., C. Nau, and G. K. Wang. 2000. Residues in Na(+) channel D3–S6 segment modulate both batrachotoxin and local anesthetic affinities. *Biophys. J.* 79:1379–1387.

Wang, S.-Y., and G. K. Wang. 1997. A mutation in segment I-S6 alters slow inactivation of sodium channels. *Biophys. J.* 72:1633–1640.

Wang, S.-Y., and G. K. Wang. 1998. Point mutations in segment I-S6 render voltage-gated Na+ channels resistant to batrachotoxin. *Proc. Natl. Acad. Sci. U.S.A.* 95:2653–2658.

Wang, S.-Y., and G. K. Wang. 1999. Batrachotoxin-resistant Na^+ channels derived from point mutations in transmembrane segment D4–S6. *Biophys. J.* 76:3141–3149.

Wang, D. W., K. Yazawa, A. L. J. George, and P. B. Bennett. 1996. Characterization of human cardiac Na^+ channel mutations in the congenital long QT syndrome. *Proc. Natl. Acad. Sci. U.S.A.* 93: 13200–13205.

Yang, N., A. L. George, and R. Horn. 1997. Probing the outer vestibule of a sodium channel voltage sensor. *Biophys. J.* 73:2260–2268.

Yarov-Yarovoy, V., J. Brown, E. M. Sharp, J. J. Clare, T. Scheuer, and W. A. Catterall. 2001. Molecular determinants of voltage-dependent gating and binding of pore-blocking drugs in transmembrane segment IIIS6 of the Na+ channel alpha subunit. *J. Biol. Chem.* 276:20–27.

Yellen, G. 1998. The moving parts of voltage-gated ion channels. *Q. Rev. Biophys.* 31:239–295.